Optics Communications 335 (2015) 16–22

Contents lists available at ScienceDirect

Optics Communications

journal homepage: www.elsevier.com/locate/optcom

Photonic band structure in one-dimensional nonlinear crystal: Analysis of harmonic stability

Carlos G. Avendaño [a,*], J. Adrián Reyes [b]

[a] Universidad Autónoma de la Ciudad de México, Av. La Corona No. 320, Col. La Palma, C.P. 07160, G. A. Madero, México D. F., Mexico
[b] Instituto de Física, Universidad Nacional Autónoma de México, Apartado Postal 20 364 01000, México D. F., México

ARTICLE INFO

Article history:
Received 30 April 2014
Received in revised form
30 July 2014
Accepted 1 August 2014
Available online 14 August 2014

Keywords:
Nonlinear optics
Photonic crystal
Stability
Nonlinear band structure

ABSTRACT

We consider a one-dimensional nonlinear photonic crystal consisting of an infinite set of concentrated equidistant scatterers inserted in a linear dielectric medium. Each of the scatterers is made by a very thin layer of a nonlinear medium with high refractive index that we model by a delta function. We show that the nonlinear optical exact solutions of this system form an intensity dependent band structure. To analyze the stability of these solutions we consider a modulation harmonic perturbation of these solutions whose amplitudes are slightly above the instability threshold. We demonstrate that the nonlinearity gives rise to an oscillatory instability of the solutions, which is a localized version of the well-known modulational instability of the nonlinear Schrodinger equation. We show that the linear harmonic perturbation forms as well a band structure whose allowed bands coincide for some intervals with those of the nonlinear band structure of the solutions for which case the structures are unstable whereas in the region where both the linear and nonlinear bands do not coincide, the nonlinear waves are indeed stable so that they conform spatial solitons.

© 2014 Elsevier B.V. All rights reserved.

1. Introduction

It is well known that spatially periodic dielectric structures can exhibit photonic band gap structures for light propagation, for which, any wave whose frequency lies within such a band gap will suffer Bragg reflection and no transmission of light will be there; property that can be used in many potential applications [1]. In several of these systems, external agents, such as pressure, heat or electromagnetic fields, have been used to change their optical properties. Two classes of tunable properties in periodic structures can be distinguished. In the first one, an external agent causes structural changes with no alteration of the dielectric constants of the constituent materials [2]. In the second one, the configuration of the structure remains the same and it is some material property that changes by the action of the external agent, including the nonlinear influence of propagating electromagnetic waves through the medium [3]. The theoretical and experimental study of nonlinear wave phenomena in natural and artificial periodic structures has been matter of interest in the scientific community during decades. Optical solitons appear in a structure if the nonlinear waves propagating in it maintain their shape while they travel through the medium due to balance between the dispersion and the nonlinearity. Analysis of one-dimensional and multidimensional optical solitons in periodic dielectric structures is a growing area due to their many interesting properties and potentially useful applications. In 1987, Chen and Mills [4] studied theoretically the standing-wave (immobile) optical solitons through superlattices of finite length for incident radiation with its frequency within the forbidden band. They demonstrated that when such a system is illuminated under this condition, increasing power can switch it from a state with low transmissivity to a state with transmissivity of unity. Later, in Refs. [5,6] nonstationary (mobile) optical solitons in Kerr-nonlinear periodic structures were showed even though the power spectra of the waves lie well within the frequency band gap of the periodic structure. In 1996, the first experimental observation of soliton propagation in fiber Bragg gratings [7] was reported. Resonantly absorbing Bragg reflector (RABR) is a periodic structure composed of thin layers of resonant two-level systems separated by half-wavelength nonabsorbing dielectric layers. Kozhekin and Kurizki [8] have shown that pulse transmission through RABR can produce self-induced transparency in the band gap of such structures. In Ref. [9] was demonstrated that such a system gives rise to a vast family of stable bright gap solitons, both standing and moving. Subsequently, it was predicted that, depending on the initial conditions, stable dark and bright solitons for the same values of the parameters can be supported in RABR [10]. This analysis showed

* Corresponding author. Tel.: +52 55 58501901x18284.
E-mail address: caravelo2000@gmail.com (C.G. Avendaño).

http://dx.doi.org/10.1016/j.optcom.2014.08.001
0030-4018/© 2014 Elsevier B.V. All rights reserved.

that, depending on the parameter's values, the frequency band of the quiescent dark solitons coexists with one or two bands of the stable bright ones, without an overlap. Stability of dark-soliton solutions against arbitrary small perturbations was also illustrated.

Nonlinear periodic systems, such as optical structures and Bose–Einstein Condensates (BECs), are often described by the nonlinear Schrödinger equation combined with an external potential. Li and Smerzi [11] studied the nonlinear Schrödinger equation with an external Kronig–Penney potential, given by a periodic array of delta-functions. They found analytical solutions of zero-current states having the same or a different periodicity of the potential and studied the chemical potential dependence of nonlinear Bloch states. The authors in Ref. [12] have considered a model combining the external Kronig–Penney potential, in the form of a periodic array of rectangular potential wells, and the cubic-quintic nonlinearity. The system supports a plethora of soliton states, including fundamental single-humped solitons, symmetric and antisymmetric double-humped ones, and three-peak solitons with and without the phase shift π between the peaks. Also, the computation of stability eigenvalues and direct simulations of perturbed solitons demonstrated that they all are stable. Recently, Dror and Malomed [13] considered a model based on an external cosine-type potential, with the nonlinearity (attractive or repulsive) concentrated either at a single point or at a symmetric set of two points, which are represented, respectively, by one or two delta functions. With the attractive or repulsive sign of the nonlinearity, this model produces ordinary solitons or gap solitons, which lie, respectively, in the semi-infinite or finite gaps of the system's linear spectrum, being pinned to the delta functions. They demonstrated that the single delta function multiplying the nonlinear term supports families of stable regular solitons in the self-attractive case, while a family of solitons supported by the attractive delta function in the absence of the periodic potential is completely unstable. Also, they exhibited that the delta function can support stable gap solitons in the first finite band gap. In the model with the symmetric set of two delta functions, they studied the effect of the spontaneous symmetry breaking of the pinned solitons. Two configurations were discussed, with the delta functions set symmetrically with respect to the minimum or maximum of the underlying periodic potential. In Ref. [14] an optical periodic system formed by an infinite succession of very thin nonlinear interfaces modeled individually by delta functions, immersed in a host linear medium, was regarded. They calculated analytically the band structure of the system as a function of the incident wave intensity, finding the appearance of prohibited bands and, the separation and narrowing of these bands. To some extent, the model considered in Ref. [14] represents an extension of the investigation analyzed in Ref. [13] without including the periodic potential.

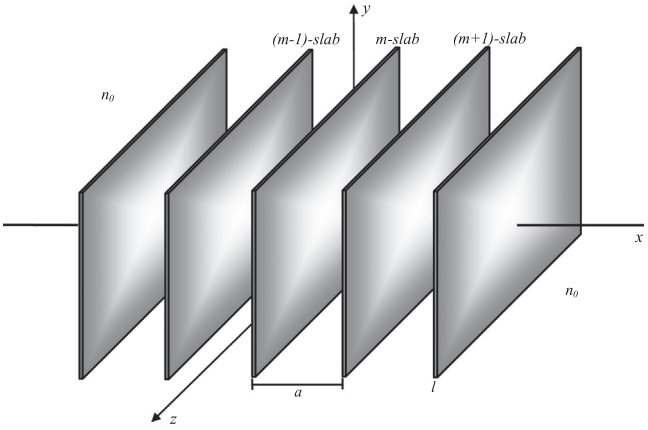

Fig. 1. The schematics of our nonlinear model.

Our research is focused on two main objectives. The first one is to obtain analytically the nonlinear optical solutions of the same structure considered in Ref. [14], which conform a photonic band structure that can be controlled by the intensity of the incident wave beam. In the second aim, by adding small harmonic perturbations to the nonlinear exact solutions, we analyze the stability of the nonlinear wave. Here, we consider that the nonlinear interfaces are made of a soft matter medium whose nonlinear response is that of a Kerr material for which the nonlinear response is proportional to the square of the magnitude of the intensity of the light [15]. The system studied here can be achieved by alternating extremely thin slabs of a soft matter material like a nematic liquid crystal with thicker solid state films. Hence, for a low power laser beam (for instance He–He) the nonlinear refractive index of the solid stacks is to be negligible in comparison with that of the nematic films whose typical value is more than eight orders of magnitude larger than that of a solid dielectric medium [16]. The structure of our paper is as follows. In Section 2, we implement a theoretical model for this one-dimensional crystal. From the wave equation and their corresponding periodic boundary condition, we calculate the dispersion relation to obtain the band structure. In Section 3 we analyze the stability of the exact solutions in the intensity dependent band structure by including a small disturbance whose strength is above the threshold activation value. In Section 4 we discuss our conclusions.

2. One-dimensional nonlinear photonic crystal

We consider a one-dimensional photonic crystal made by an infinite set of very thin nonlinear layers inserted in a linear host medium (see Fig. 1). If we neglect the thicknesses of the slabs and we take their nonlinear refractive index high enough in comparison to that of the linear medium, we can represent each of these slabs by a delta potential whose amplitude is a function of the intensity of the field. In this sense, we can assume a nonlinear relative permittivity function in the form

$$\epsilon_r(x) = \epsilon_{0r} + (\alpha_1 + \alpha_2(|E_y|^2 + |E_z|^2))\delta(x - ma), \tag{1}$$

where $\epsilon_{0r} = n_0^2$ is the square root of the refractive index of the linear medium, $\alpha_1 = \lim(\epsilon_{1r} l)_{\epsilon_{1r}\to\infty, l\to 0}$ and $\alpha_2 = \lim(\epsilon_{2r} l)_{\epsilon_{2r}\to\infty, l\to 0}$ are the linear and nonlinear coefficients, respectively, that determine the strength of the delta function, $\epsilon_{1r} = n_1^2$ and $\epsilon_{2r} = n_2^2$ are the square roots of the refractive indices related to the linear and nonlinear responses inside the extremely little thickness stacks, E is the electric field amplitude, $\delta(x)$ is Dirac's delta function, a is the separation between scatterers and represents the spatial periodicity of the system, $x = ma$ indicates the position of each layer and m is an integer number to numerate the nonlinear slabs. Here, we have assumed a Kerr-type response of the nonlinear medium.

If we suppose a propagating wave of the form $(H_z(x,t), E_z(x,t)) = (H_z(x), E_z(x))\exp(-i\omega t)$, we can write the curl Maxwell equations as

$$\frac{\partial E_z}{\partial \chi} = -i\omega\mu_0 a H_y, \tag{2}$$

$$\frac{\partial H_y}{\partial \chi} = -i\epsilon_0\omega a E_z[n_0^2 + (\alpha_1 + \alpha_2(|E_y|^2 + |E_z|^2))\sum\delta(\chi - m)/a], \tag{3}$$

$$\frac{\partial E_y}{\partial \chi} = i\omega\mu_0 a H_z, \tag{4}$$

$$\frac{\partial H_z}{\partial \chi} = i\epsilon_0\omega a E_y[n_0^2 + (\alpha_1 + \alpha_2(|E_y|^2 + |E_z|^2))\sum\delta(\chi - m)/a], \tag{5}$$

where $\chi = x/a$ and we have used the property $\delta(ax) = \delta(x)/a$. To discern the influence of this function on the solutions let us deduce the corresponding boundary conditions by integrating Eqs. (2) and (4) across the nonlinear slabs situated at $\chi = m$. It gives

$$H_y((m+1)^+) - e^{-if} H_y(m^-) = -i\epsilon_0 \omega E_z(\alpha_1 + \alpha_2(|E_y|^2 + |E_z|^2))(m^+),$$
$$E_z((m+1)^+) = e^{-if} E_z(m^-), \tag{6}$$

$$H_z((m+1)^+) - e^{-if} H_z(m^-) = i\epsilon_0 \omega E_y(\eta_1^2 E_y + \Delta E_y |E_y^2|)(m^+),$$
$$E_y((m+1)^+) = e^{-if} E_y(m^-), \tag{7}$$

where we have used the Bloch theorem which states that $(H_z(\chi + m), E_z(\chi + m)) = e^{-if}(H_z(\chi), E_z(\chi))$; f is the Bloch parameter which characterizes the momentum of the associated unit cell. These expressions can be written only in terms of electric field components and their derivatives as

$$\frac{dE_z}{d\chi}((m+1)^+) - e^{-if}\frac{dE_z}{d\chi}(m^-) = -k_0^2 a E_z(\alpha_1 + \alpha_2(|E_y|^2 + |E_z|^2))(m^+), \tag{8}$$

$$E_z((m+1)^+) = e^{-if} E_z(m^-), \tag{9}$$

$$\frac{dE_y}{d\chi}((m+1)a^+) - e^{-if}\frac{dE_y}{d\chi}(m^-) = -k_0^2 a E_y(\alpha_1 + \alpha_2(|E_y|^2 + |E_z|^2))(m^+), \tag{10}$$

$$E_y((m+1)^+) = e^{-if} E_y(m^-), \tag{11}$$

The general solutions of Eqs. (2)–(5) are given by

$$(E_y, E_z) = \{A\cos\ k\chi + B\ \sin\ k\chi,\ C\cos\ k\chi + D\ \sin\ k\chi\}, \tag{12}$$

where A, B, C, and D are constants to be determined by the boundary conditions and $k = k_0 a$. If we insert Eq. (12) into Eqs. (8)–(11) we get

$$A - e^{-if}(A\cos\ k + B\ \sin\ k) = 0, \tag{13}$$

$$Bk - e^{-if}k(B\cos\ k - A\ \sin\ k) = -\frac{k^2}{a}(\alpha_1 A + \alpha_2 A(|A|^2 + |C|^2)), \tag{14}$$

$$C - e^{-if}(C\cos\ k + D\ \sin\ k) = 0, \tag{15}$$

$$Dk - e^{-if}k(D\cos\ k - C\ \sin\ k) = -\frac{k^2}{a}(\alpha_1 C + \alpha_2 C(|A|^2 + |C|^2)). \tag{16}$$

Now, by solving Eq. (13) for B, we get the expression $B = A(e^{if} - \cos\ k)/\sin\ k$ that can be substituted into Eq. (14) to yield

$$\frac{Ak(e^{if} - \cos\ k)}{\sin\ k} - e^{-if}k\left(\frac{A(e^{if} - \cos\ k)}{\sin\ k}\cos\ k - A\sin\ k\right) = -\frac{k^2 A}{a}(\alpha_1 + \alpha_2(|A|^2 + |C|^2)). \tag{17}$$

Then, we multiply by $\sin\ k/Ak$ to obtain

$$e^{if} - \cos\ k - (\cos\ k - e^{-if}\ \cos^2 k - e^{-if}\ \sin^2 k) = -\frac{k}{a}(\alpha_1 + \alpha_2(|A|^2 + |C|^2))\sin\ k, \tag{18}$$

that can be expressed as

$$\cos\ f = \cos\ k - (g_l + g_{nl} + h_{nl})\frac{k\ \sin\ k}{2}, \tag{19}$$

where $g_l = \alpha_1/a$, $g_{nl} = \alpha_2|A|^2/a$ and $h_{nl} = \alpha_2|C|^2/a$. The fact that $|\cos f| \le 1$ implies that the values of k satisfying Eq. (19) are limited to those ones for which the absolute value of the right hand side is also smaller than or equal to one. If we define the function $u(k) = \cos\ k - \frac{1}{2}(g_l + g_{nl} + h_{nl})k\ \sin\ k$, then the condition,

$$|u(k)| \le 1, \tag{20}$$

gives all the permitted k values for which the expression (12) is the solution of the set (2)–(5). By solving for the other two expressions C, D, we obtain exactly the same expression. Here we consider that only the E_y component is present; this means that $h_{nl} = 0$. A plot of $u(k)$ is shown in Fig. 2 for specific values of g_{nl} where the allowed k bands are the regions of the curve lying between the horizontal lines $u = 1$ and $u = -1$. It can be observed that the thicknesses of the permitted (forbidden) bands thin (thicken) as the wave amplitude increases. We have depicted in Fig. 3a three-dimensional graph of u as a function of $k = k_0 a$ and g_{nl}. The dark regions of the surface standing outside the region $-1 \le u \le 1$ are the forbidden bands whose thicknesses increase as the wave amplitude grows. Notice that, if we take $g_{nl} = h_{nl} = 0$, expression (20) corresponds to that obtained in the case of the linear Schrödinger equation with a delta-Kronig–Penney potential [17] (solid line in Fig. 2) showing the consistency of our calculation.

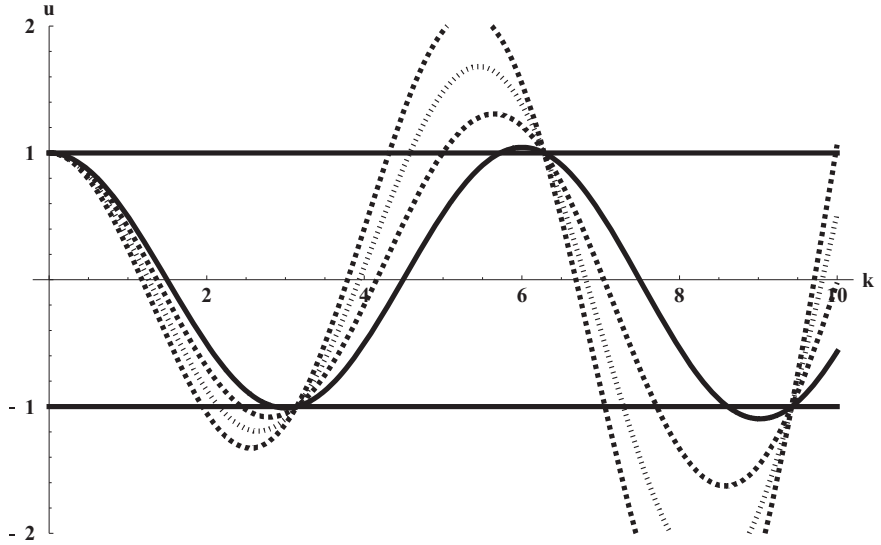

Fig. 2. Plot of $u = \cos\ f$ vs k, parametrized by the nonlinear parameter g_{nl} for values equal to 0 (solid line), 0.2 (dashed line), 0.4 (dotted line) and 0.6 (dot-dashed line). Here $g_l = 0.1$. The horizontal lines $u = 1, -1$ represent the limit between the permitted and forbidden bands.

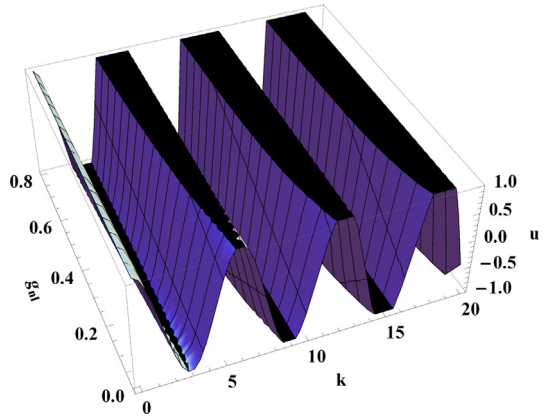

Fig. 3. 3D plot of $u=\cos f$ vs (k,g_{nl}). Here $g_l=0.1$. Dark regions of the surface standing outside the region $-1\le u\le 1$ are the forbidden bands.

3. Instability

Let us analyze the stability of the nonlinear band structure we just found in the last section. To this end we shall assume the following form for the electric field:

$$E_z=e^{-i\omega t}(A\cos\ k_0x+B\ \sin\ k_0x)+\psi_1(x,t)=\psi_0(x,t)+\psi_1(x,t), \tag{21}$$

where $\psi_1(x,t)$ denotes a small linear harmonic perturbation to the nonlinear solution, whereas ψ_0 stands for the stationary solution whose permitted band structure is described by Eq. (20). The direct substitution of this field into Maxwell's equations leads to

$$\frac{\partial(\psi_0(x,t)+\psi_1(x,t))}{\partial\chi}=a\mu_0\frac{\partial H_y}{\partial t}, \tag{22}$$

$$\frac{\partial H_y}{\partial\chi}=a\epsilon_0\frac{\partial(\epsilon_r(\chi)(\psi_0(\chi,t)+\psi_1(\chi,t)))}{\partial t}, \tag{23}$$

where $\chi=x/a$ and

$$\epsilon_r(\chi,t)=n_0^2+(\alpha_1+\alpha_2(|\psi_0(\chi,t)+\psi_1(\chi,t)|^2))\delta(\chi-m)/a. \tag{24}$$

If we keep only terms up to first order in $\psi_1(\chi,t)$ we get

$$\frac{\partial\psi_1(\chi,t)}{\partial\chi}=a\mu_0\frac{\partial H_y}{\partial t}, \tag{25}$$

$$\frac{1}{a\epsilon_0}\frac{\partial H_y}{\partial\chi}=\frac{\partial}{\partial t}\{(n_0^2+(\alpha_1+\alpha_2|\psi_0|^2)\sum\delta(\chi-m)/a)\psi_1 +\alpha_2(\psi_1|\psi_0|^2+\psi_0^2\psi_1^*)\sum\delta(\chi-m)/a\}. \tag{26}$$

We can combine expressions (25) and (26) to obtain

$$\frac{1}{a^2\epsilon_0\mu_0}\frac{\partial^2\psi_1}{\partial\chi^2}=\frac{\partial^2}{\partial t^2}\{(n_0^2+(\alpha_1+\alpha_2|\psi_0|^2)\sum\delta(\chi-m)/a)\psi_1 +\alpha_2(\psi_1|\psi_0|^2+\psi_0^2\psi_1^*)\sum\delta(\chi-m)/a\}. \tag{27}$$

If we integrate this expression around the nonlinear slab located at $\chi=0$ and we take into account that the stationary solution can be written as $\psi_0(\chi,t)=e^{-i\omega t}(A\cos\ k\chi+B\ \sin\ k\chi)$, we get

$$\frac{c^2}{a}\left(\frac{\partial\psi_1(0,t)}{\partial\chi}-e^{-i\theta}\frac{\partial\psi_1(1,t)}{\partial\chi}\right)= \frac{\partial^2}{\partial t^2}\left\{\alpha_1\psi_1(0,t)+A^2\alpha_2(2\psi_1(0,t)+\psi_1^*(0,t)e^{-2i\omega t})\right\}, \tag{28}$$

where θ is the Bloch phase of the perturbation and we $c^2=1/\epsilon_0\mu_0$. Next, we propose a solution for $\psi_1(\chi,t)$ of the form

$$\psi_1(\chi,t)=e^{-i\Omega t+\Gamma t}\phi_1(\chi)+e^{-i(2\omega-\Omega)t+\Gamma t}\phi_2^*(\chi), \tag{29}$$

where $\phi_1(\chi)$ and $\phi_2^*(\chi)$ are functions containing the spatial dependence of these linear perturbations and Ω, $2\omega-\Omega$ are the harmonic frequencies of the same harmonic components. Here Γ is a parameter controlling the size of the harmonic perturbation. Then inserting these two expressions in the boundary condition equation (28), and arguing linear independence between harmonics Ω, $2\omega-\Omega$, we can separate this expression into two independent expressions:

$$\frac{c^2}{a}\left(\frac{\partial\phi_1(0)}{\partial\chi}-e^{-i\theta}\frac{\partial\phi_1(1)}{\partial\chi}\right)=(\Gamma-i\Omega)^2(\alpha_1+2A^2\alpha_2)\phi_1(0) +A^2\alpha_2(\Gamma-i\Omega+2i\omega)^2\phi_2(0), \tag{30}$$

$$\frac{c^2}{a}\left(\frac{\partial\phi_2^*(0)}{\partial\chi}-e^{-i\theta}\frac{\partial\phi_2^*(1)}{\partial\chi}\right)=(\Gamma+i\Omega-2i\omega)^2(\alpha_1+2A^2\alpha_2)\phi_2^*(0) +A^2\alpha_2(\Gamma+i\Omega)^2\phi_1^*(0). \tag{31}$$

In addition to this, we need to ask also for the continuity of the functions together with the Bloch theorem as

$$\phi_1(0)-e^{-i\theta}\phi_1(1)=0, \tag{32}$$

$$\phi_2^*(0)-e^{-i\theta}\phi_2^*(1)=0. \tag{33}$$

Then, we are to choose the functions $\phi(\chi)$ as the harmonic combinations

$$\phi_1=C\ \cos(p+i\gamma)\chi+D\ \sin(p+i\gamma)\chi, \quad \phi_2=F\ \cos(q+i\lambda)\chi+G\ \sin(q+i\lambda)\chi, \tag{34}$$

where C, D, F and G are constants to be determined from the boundary conditions. Here $p+i\gamma$ and $q+i\lambda$ are complex wave numbers associated to the harmonic perturbations. The substitution of these expressions into Eqs. (30)–(33) gives the following set of equations:

$$\frac{c^2e^{-i\theta}(p+i\gamma)(De^{i\theta}-D\ \cos(p+i\gamma)+C\ \sin(p+i\gamma))}{a} =C(\alpha_1+2A^2\alpha_2)(\Gamma-i\Omega)^2+FA^2\alpha_2(\Gamma+2i\omega-i\Omega)^2, \tag{35}$$

$$\frac{c^2e^{-i\theta}(q-i\lambda)(Ge^{i\theta}-G\ \cos(q-i\lambda)+F\ \sin(q-i\lambda))}{a} =CA^2\alpha_2(\Gamma+i\Omega)^2+F(\alpha_1+2A^2\alpha_2)(\Gamma-2i\omega+i\Omega)^2, \tag{36}$$

$$C=e^{-i\theta}(C\ \cos(p+i\gamma)+D\ \sin(p+i\gamma)), \tag{37}$$

$$F=e^{-i\theta}(F\ \cos(q-i\lambda)+G\ \sin(q-i\lambda)). \tag{38}$$

Now, we eliminate from the two last equations D and G to reduce the system to only two equations for the constants C and F, it yields

$$-\frac{2c^2C(p+i\gamma)(\cos(p+i\gamma)-\cos\ \theta)\csc(p+i\gamma)}{a} =C(\alpha_1+2A^2\alpha_2)(\Gamma-i\Omega)^2+FA^2\alpha_2(\Gamma+2i\omega-i\Omega)^2, \tag{39}$$

$$-\frac{2c^2F(q+i\lambda)(\cos(q-i\lambda)-\cos\ \theta)\csc(q-i\lambda)}{a} =A^2C\alpha_2(\Gamma+i\Omega)^2+F(\alpha_1+2A^2\alpha_2)(\Gamma-2i\omega+i\Omega)^2. \tag{40}$$

Some other complementary relations among the parameter involved are coming from the substitution of Eqs. (29) and (34) into Eq. (27) for $\chi\neq m$; it allows us to write

$$\frac{c^2}{a^2}(p+i\gamma)^2=-n_0^2(\Gamma-i\Omega)^2, \quad \frac{c^2}{a^2}(q-i\lambda)^2=-n_0^2(\Gamma-i(2\omega-\Omega))^2, \tag{41}$$

or equivalently

$$p=\frac{an_0}{c}\Omega; \quad q=\frac{an_0}{c}(\Omega-2\omega); \quad \gamma=\lambda=\frac{an_0}{c}\Gamma. \tag{42}$$

To find a nontrivial solution of the set of Eqs. (39) and (40) we ask for a vanishing value of its determinant, it gives

$$\cos^2\theta+(r_1+is_1)\cos\theta+r_0+is_0=0, \tag{43}$$

where

$$r_1=\mathrm{Re}[\beta_1],\quad s_1=\mathrm{Im}[\beta_1],$$
$$r_0=\mathrm{Re}[\beta_0],\quad s_0=\mathrm{Im}[\beta_0], \tag{44}$$

Re[z] and Im[z] denote the real and the imaginary part of the complex number z, respectively, and

$$\beta_1=\frac{(q-i\lambda)(-2c^2(p+i\gamma)\cos(p+i\gamma)-a(\alpha_1+2A^2\alpha_2)(\Gamma-i\Omega)^2\sin(p+i\gamma))}{2c^2(p+i\gamma)(q-i\lambda)}$$
$$+\frac{(p+i\gamma)(-2c^2(q-i\lambda)\cos(q-i\lambda)-a(\alpha_1+2A^2\alpha_2)(\Gamma-2i\omega+i\Omega)^2\sin(q-i\lambda))}{2c^2(p+i\gamma)(q-i\lambda)}, \tag{45}$$

$$\beta_0=\frac{\sin(p+i\gamma)\sin(q-i\lambda)}{4c^4(p+i\gamma)(q-i\lambda)}$$
$$\{[\alpha_1(\Gamma^2-2i\Gamma\omega+\Omega(-2\omega+\Omega))+A^2\alpha_2(\Gamma^2-6i\Gamma\omega$$
$$+\Omega(-2\omega+\Omega))][\alpha_1(\Gamma^2-2i\Gamma\omega+\Omega(-2\omega+\Omega))$$
$$+A^2\alpha_2(3\Gamma^2-2i\Gamma\omega+3\Omega(-2\omega+\Omega))]$$
$$+2c^2[a(\alpha_1+2A^2\alpha_2)(q-i\lambda)(\Gamma-i\Omega)^2\cot(q-i\lambda)$$
$$+(p+i\gamma)\cot(p+i\gamma)(a(\alpha_1+2A^2\alpha_2)(\Gamma-2i\omega+i\Omega)^2$$
$$+2c^2(q-i\lambda)\cot(q-i\lambda))]\}. \tag{46}$$

Notice that the values of parameters p, q, γ and λ in terms of ω, Ω, Γ are determined in Eqs. (42).

By solving expression (43) for $\cos\theta$, we find

$$\cos\theta=\frac{-(r_1+is_1)\pm\sqrt{u+iv}}{2}, \tag{47}$$

where $u=r_1^2-s_1^2-4r_0$ and $v=2r_1s_1-4s_0$. It is useful to separate the real and the imaginary part of this solution to get

$$\mathrm{Re}[\cos\theta]=-\frac{r_1}{2}-\sqrt{\frac{1}{8}(\sqrt{u^2+v^2}+u)}, \tag{48}$$

$$\mathrm{Im}[\cos\theta]=-\frac{s_1}{2}+\sqrt{\frac{1}{8}(\sqrt{u^2+v^2}-u)}. \tag{49}$$

It is required that θ be a real quantity, in such a way that we ask for the imaginary part of $\cos\theta$ equal to zero. This condition allows to write the following relation:

$$rs_1^2+s_0^2-r_1s_0s_1=0. \tag{50}$$

which relates the parameters ω, Ω, Γ and the material parameters of the medium. We are interested in analyzingthe threshold in which the harmonic perturbation is activated. For this purpose, we expand Eq. (50) in the Taylor series up to second order in Γ around zero. We find an expression of the form

$$\mathrm{Im}[\cos\theta]=\cos f(\omega,\Omega)\Gamma^2+O(\Gamma)^3. \tag{51}$$

Hence for a very small Γ, ω and Ω are related by the expression $\cos f(\omega,\Omega)=0$. We solve numerically this transcendental equation for Ω by providing specific given values of $\{\omega\}$ and the material parameters α_1, α_2, n_0, a, and amplitude A. On the other side, we substitute Eqs. (44) in Eq. (48) and set $\Gamma=0$ to obtain the expression for the harmonic perturbation only in terms on ω and Ω, this means that

$$\mathrm{Re}[\cos\theta]=\mathrm{Re}[\cos\theta(\omega,\Omega(\omega))]. \tag{52}$$

A nontrivial exact solution for expression $\cos f(\omega,\Omega)=0$ is found to be $\Omega=2\omega$, independently of material parameters, such that Eq. (52) can be written as

$$\mathrm{Re}[\cos\theta]=\frac{1}{2}+\frac{1}{2}\cos 2kn_0-\frac{(g_l+2g_{nl})k\sin 2kn_0}{2n_0}$$
$$-\frac{|\sin kn_0((g_l+2g_{nl})k\cos kn_0+n_0\sin kn_0)|}{n_0}. \tag{53}$$

where k, g_l and g_{nl} are defined as in Eq. (19) and $|z|$ represents the absolute value of z. As before, since $|\mathrm{Re}[\cos\theta]|\le 1$, the condition

$$\left|\frac{1}{2}+\frac{1}{2}\cos 2kn_0-\frac{(g_l+2g_{nl})k\sin 2kn_0}{2n_0}\right.$$
$$\left.-\frac{|\sin kn_0((g_l+2g_{nl})k\cos kn_0+n_0\sin kn_0)|}{n_0}\right|\le 1, \tag{54}$$

gives all the allowed k values for which the expression (29) is a solution of the linear perturbation. We depict the function Re[$\cos\theta(k)$] in Fig. 4 for three different values of nonlinear parameter g_{nl}. The permitted solutions are those belonging to the interval for which the right-hand side function remains in the interval $[-1,1]$. The set of all these solutions forms the linear band structure of the harmonic perturbation. This implies that not only the set of nonlinear solutions conforms a band structure but also a

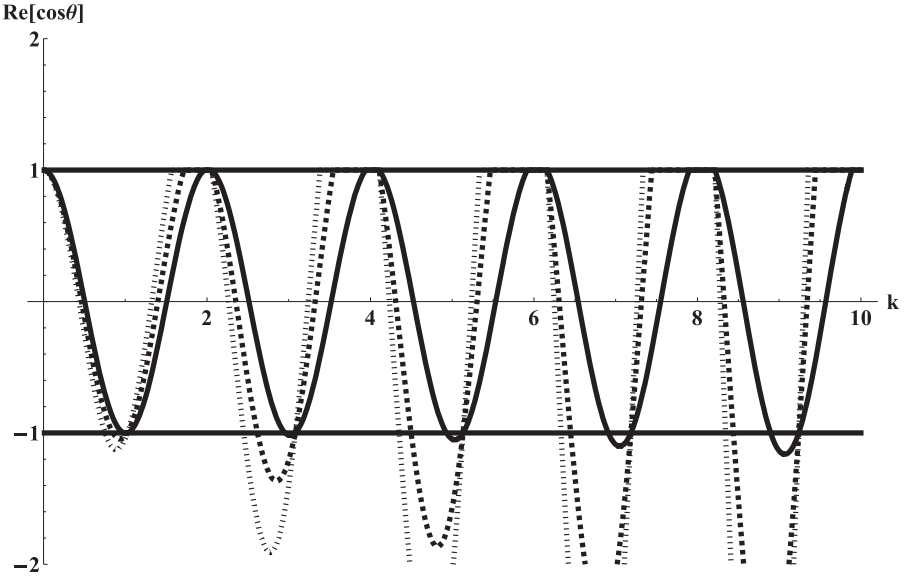

Fig. 4. Plot of linear disturbance band structure Re[$\cos\theta$] vs k parametrized by the nonlinear parameter g_{nl} for values equal to 0 (solid line), 0.2 (dashed line), and 0.4 (dotted line). Here $g_l=0.1$.

harmonic small perturbation. In this way the places where both band structures coincide correspond to states in which the solutions are unstable whereas the rest of the states are stable. Also, notice that, as in the nonlinear band structure case, the thicknesses of the permitted (forbidden) bands thin (thicken) as the amplitude gets larger. In Fig. 5 we show the nonlinear and linear band structures for a specific value. The nonlinear band structure is represented by the function $u(k) = \cos f$ as defined in Eq. (19), whereas the linear disturbance band one is given by $\mathrm{Re}[\cos\theta(k)]$ as expressed in Eq. (53). The regions where both functions remain in the interval $[-1, 1]$ are represented by a thick solid line along the k-axis. These zones correspond to unstable solutions as a function of k. The origin of the instability in these intervals is the same lack of balance between spatial dispersion and nonlinearity associated to the standard nonlinear Schrodinger equation.

Conversely, the regions for which there exist nonlinear wave bands, but there are forbidden bands for the harmonic perturbations, are regions of robust stable nonlinear waves called spatial solitons [18]. We can describe the band structure we just calculated in the following way. It contains three types of bands: the forbidden bands in which no wave can be propagated, the unstable nonlinear wave bands for which the waves are unstable under harmonic oscillations, and the soliton bands for which the small harmonic disturbance is damped leaving only the robust spatial coherent structures. It is worth noticing that, unlike Ref. [13], where a family of solitons supported by the attractive delta function in the absence of the periodic potential are completely unstable, our nonlinear infinite periodic system can support, under certain conditions, solutions completely stable. In Fig. 6, for specific values of k, we plot the nonlinear solutions of electric field, given by expression $E_z(\chi, t) = e^{-i\omega t}(A\cos k\chi + B\sin k\chi)$, which satisfy the set of Eqs. (2)–(5) and subjected to a small harmonic perturbation as expressed in Eq. (29). As discussed above, there are intervals of k for which the nonlinear waves constitute stable or unstable solitons. For the specific value $k=4.66$, the upper figure demonstrates the evolution of a stable soliton and, for $k=2.15$, the lower figure shows the development of an unstable soliton. Notice that the upper shape has more "humps" with respect to that of the lower shape. This is because, for the former case, we have chosen a k value within the second nonlinear band (see dashed line of Fig. 5), whereas for the latter case a k value within the first nonlinear band was selected. Higher values of k correspond to higher frequencies ω and therefore, it implies a higher energy of the wave.

4. Concluding remarks

We have considered a model for a nonlinear media where the nonlinearity is Kerr-like and concentrated in an infinite number of equidistant very thin slabs, whereas the rest of the medium is linear. We have calculated analytically the optical solutions of the system which conforms a band structure depending on intensity of

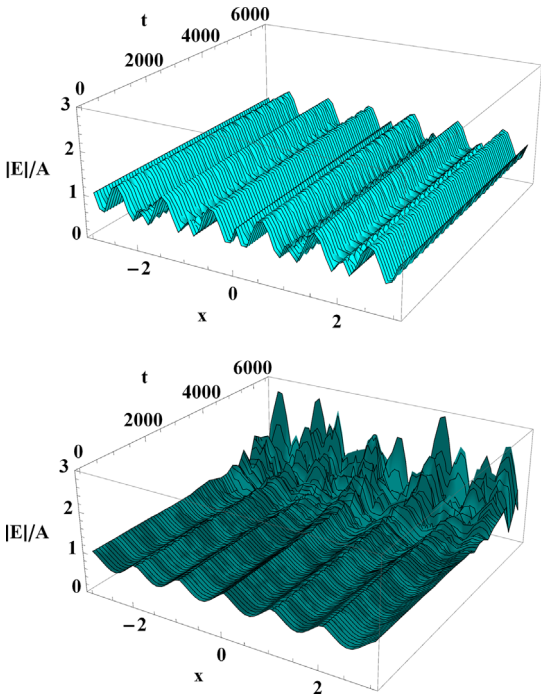

Fig. 6. The evolution of a stable soliton for $k=4.66$ (upper shape) and an unstable soliton for $k=2.15$ (lower shape) subjected to a small harmonic perturbation. The electric field E_z is normalized to the incident amplitude A. The nonlinear slabs are situated at $\chi = m$, where m is an integer number. As in Fig. 5, we have chosen $g_l = 0.1$ and $g_{nl} = 0.2$. Also, $a = 1\times10^{-6}$ m and $n_0 = 1.53$.

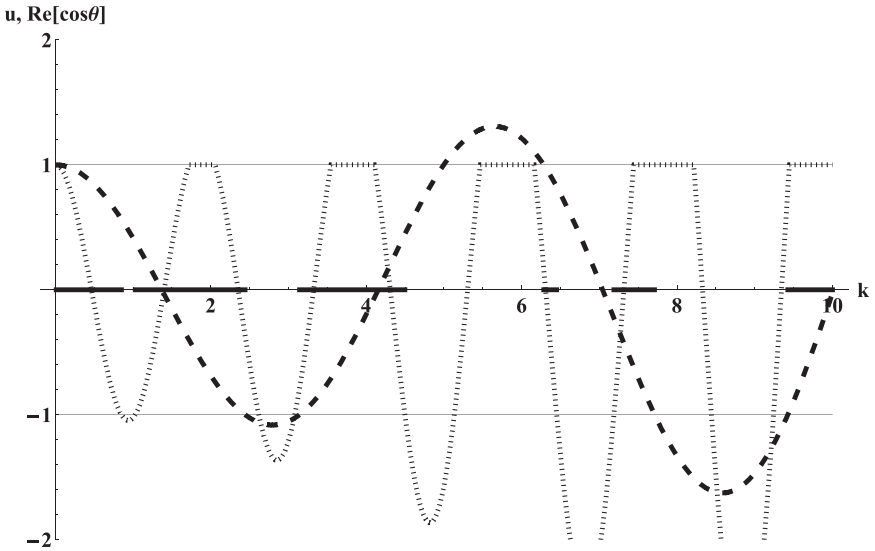

Fig. 5. Plot of (u, $\mathrm{Re}[\cos\theta]$) vs k for $g_l = 0.1$ and $g_{nl} = 0.2$. The nonlinear band structure is represented by function $u = \cos f$ (dashed line), whereas the linear disturbance band one is given by $\mathrm{Re}[\cos\theta]$ (small dashed line). Thick solid line along the k-axis indicates the unstable solutions dependent on k.

the beam. We have added small harmonic perturbations to the nonlinear solutions in order to analyze the stability of the nonlinear wave. We have found that this linear disturbance form a different band structure for the linear disturbance. This means that not only the set of solutions constitutes a band structure but also the harmonic small perturbation has a different one. Therefore, the regions where both permitted band structures concur correspond to states in which the nonlinear waves are unstable while the existing waves standing in the forbidden bands of the small perturbation are stable solutions and as a consequence they constitute spatial solitons. The origin of the stability in the corresponding intervals is caused by a similar balance between the spatial dispersion and the nonlinearity giving rise to self-focusing, associated to the well-known nonlinear Schrödinger equation.

We have demonstrated that in general, for both kinds of band structures, the thicknesses of the permitted (forbidden) bands thin (thicken) as the electromagnetic wave amplitude increases. We hope that our theoretical research contributes to increase the interest and construction on these hybrid structures for which we have demonstrated the existence of band structure of spatial solitons combined with bands of nonlinear unstable waves upon harmonic perturbations. One of the widely known applications of spatial solitons is their use to store optical information. In this sense this kind of crystal can be used to fabricate a device where two types of memory can be registered, one transient (with limited life time) where there are bands of nonlinear unstable spatial structure, and the other permanent for which the spatial structures conform solitons and thus are stable under temporal perturbation.

Acknowledgments

We gratefully acknowledge partial financial support from Grant DGAPA UNAM IN110012-3.

References

[1] S.L. Chuang, Physics of Photonic Devices, John Wiley & Sons, New Jersey, 2000.
[2] M. Golosovsky, Y. Saado, D. Davidov, Appl. Phys. Lett. 75 (1999) 4168;
Y. Saado, M. Golosovsky, D. Davidov, A. Frenkel, Phys. Rev. B 66 (2002) 195108.
[3] C.S. Kee, J.E. Kim, H.Y. Park, Phys. Rev. E 57 (1998) 2327;
J. Zhou, C.Q. Sun, K. Pita, Y.L. Lam, Y. Zhou, S.L. Ng, C.H. Kam, L.T. Li, Z.L. Gui, Appl. Phys. Lett. 78 (2001) 661.
[4] W. Chen, D.L. Mills, Phys Rev. Lett. 58 (1987) 160.
[5] D.N. Christodoulides, R.I. Joseph, Phys. Rev. Lett. 62 (1989) 1746.
[6] A.B. Aceves, S. Wabnitz, Phys. Rev. A 141 (1989) 37.
[7] B.J. Eggleton, R.E. Slusher, C.M. Sterke, P.A. Krug, J.E. Sipe, Phys. Rev. Lett. 76 (1996) 1627.
[8] A. Kozhekin, G. Kurizki, Phys. Rev. Lett. 74 (1995) 5020.
[9] A. Kozhekin, G. Kurizki, B.A. Malomed, Phys. Rev. Lett. 81 (1998) 3647.
[10] T. Opatrný, B.A. Malomed, G. Kurizki, Phys. Rev. E 60 (1999) 6137.
[11] W. Li, A. Smerzi, Phys. Rev. E 70 (2004) 016605.
[12] I.M. Merhasin, B.V. Gisin, R. Driben, B.A. Malomed, Phys. Rev. E 71 (2005) 016613.
[13] N. Dror, B.A. Malomed, Phys. Rev. A 83 (2011) 033828.
[14] S. Gutiérrez-López, A. Castellanos-Moreno, A. Corella-Madueño, R.A. Rosas, J.A. Reyes, Opt. Commun. 285 (2012) 2439.
[15] R.W. Boyd, Nonlinear Optics, Academic Press, London, 1992.
[16] N.V. Tabiryan, A.V. Sukhov, B.Ya. Zel'dovich, Mol. Cryst. Liq. Cryst. 136 (1986) 1;
I.C. Khoo, Nonlinear optics of liquid crystals, in: E. Wolf (Ed.), Progress in Optics, North Holland, Amsterdam, 1988, pp. 107–161;
I.C. Khoo, H. Li, Appl. Phys. B 59 (1993) 573.
[17] C. Kittel, Introduction to Solid State Physics, John Wiley & Sons, USA, 1976.
[18] B.A. Malomed, Soliton Management in Periodic Systems, Springer, New York, 2006.